

Two texture zeros for Dirac neutrinos in a diagonal charged lepton basis*

Yessica Lenis¹ John D. Gómez² William A. Ponce¹ Richard H. Benavides^{2†} 

¹Instituto de Física, Universidad de Antioquia, A.A. 1226, Medellín, Colombia

²Instituto Tecnológico Metropolitano, Facultad de Ciencias Exactas y Aplicadas, Calle 73 N° 76-354 via el volador, Medellín, Colombia

Abstract: A systematic study of the neutrino mass matrix M_ν with two texture zeros in a basis that the charged leptons are diagonal, and under the assumption that neutrinos are Dirac particles is performed. Our study is conducted without any approximation, first analytically and then numerically. Current neutrino oscillation data is used in our analysis. Phenomenological implications of M_ν on lepton CP violation and neutrino mass spectrum are explored.

Keywords: neutrinos, texture zeros, Dirac particles

DOI: 10.1088/1674-1137/ad8d4a **CSTR:** 32044.14.ChinesePhysicsC.49013107

I. INTRODUCTION

Although the gauge boson sector of the Standard Model (SM) with $SU(3)_c \otimes SU(2)_L \otimes U(1)_Y$ local symmetry has been very successful [1–4], its Yukawa sector is still poorly understood. Questions related to this sector such as the total number of families in nature, the hierarchy of the charged fermion mass spectrum, the smallness of neutrino masses, the quark mixing angles, the neutrino oscillations, and the origin of CP violation, remain open questions to date in theoretical particle physics [5–10].

In the context of the SM, a neutrino flavor created by the weak interaction and associated with a charged lepton will maintain its flavor, which implies that the lepton flavor is conserved and neutrinos are massless. Moreover, recent experimental results confirm that neutrinos oscillate, and, consequently, at least two of them have non-zero masses [11–13].

Current neutrino experiments are measuring the neutrino mixing parameters with unprecedented accuracy. The next generation of neutrino experiments will be sensitive to subdominant neutrino oscillation effects that can, in principle, provide information on the yet-unknown neutrino parameters: the Dirac CP-violating phase in the Pontecorvo-Maki-Nakagawa-Sakata (PMNS) mixing matrix U_{PMNS} , the neutrino mass ordering, and the octant of the mixing angles [14–16].

To date, the solar and atmospheric neutrino oscillations have established the following values to 3 sigma of the deviation [17–19]:

$$\begin{aligned}\Delta m_{\text{atm}}^2 &= (2.47 - 2.63) \times 10^{-3} \text{eV}^2, \\ \Delta m_{\text{sol}}^2 &= (6.94 - 8.14) \times 10^{-5} \text{eV}^2 = \Delta m_{21}^2, \\ \sin^2 \theta_{\text{atm}} &= (4.34 - 6.10) \times 10^{-1} = \sin^2 \theta_{23}, \\ \sin^2 \theta_{\text{sol}} &= (2.71 - 3.69) \times 10^{-1} = \sin^2 \theta_{12}, \\ \sin^2 \theta_{\text{Reac}} &= (2.00 - 2.41) \times 10^{-2} = \sin^2 \theta_{13},\end{aligned}\quad (1)$$

which implies, among other things, that at least two neutrinos have very small but non-zero masses.

Masses of neutrinos require physics beyond the SM connected either to the existence of right-handed neutrinos and/or to the breaking of the baryon minus lepton number ($B-L$) symmetry [20]. If right-handed neutrinos exist, the Yukawa terms, after electroweak symmetry breaking, result in Dirac neutrino masses, requiring Yukawa coupling constants for neutrinos $h_\nu^\phi \leq 10^{-13}$. However, the right-handed neutrinos, singlets under the SM gauge group, can acquire large Majorana masses and render the Type I see-saw mechanism [8, 21–23] to be an appealing and natural scenery for neutrino mass generation. Another possibility is to generate neutrino masses via quantum loops [24, 25].

For Majorana fields, a process exists called neutrinoless double beta decay ($0\nu\beta\beta$), which is strongly disfavored by current experimental results ([26–28]), the reason for which the alternative is to assume that massive neutrinos must be related to Dirac fields. Therefore, for the model analyzed, we assume that Majorana masses are forbidden by some type of physical mechanism.

Received 30 May 2024; Accepted 31 October 2024; Published online 1 November 2024

* Richard H. Benavides Acknowledges Additional Financial Support from Minciencias (CD82315 CT ICETEX 2021-1080)

† E-mail: ribebenavides@gmail.com



Content from this work may be used under the terms of the Creative Commons Attribution 3.0 licence. Any further distribution of this work must maintain attribution to the author(s) and the title of the work, journal citation and DOI. Article funded by SCOAP³ and published under licence by Chinese Physical Society and the Institute of High Energy Physics of the Chinese Academy of Sciences and the Institute of Modern Physics of the Chinese Academy of Sciences and IOP Publishing Ltd

In addition to the fact that no experiment has thus far excluded the possibility of Dirac neutrino masses, several theoretical motivations exist to assume them, for example, the generation of baryon asymmetry via leptogenesis [29], alternative approaches to the see-saw mechanism [30], and the generation of radiative neutrino masses via quantum loops [31–34]. Additionally, in models derived from string theories, the Majorana masses are strongly suppressed by selection rules related to the underlying symmetries [35].

Furthermore, the use of Dirac particle fields enables us to apply the polar decomposition theorem of algebra [36], which states that any complex matrix can be decomposed into the product of a Hermitian and a unitary matrix. This decomposition reduces the number of free parameters by half in this sector because the unitary matrix can be absorbed into the singlet representations of $SU(2)_L$, that is, in the right-handed sector (a simplification that is not possible for Majorana particles [37]).

Other theoretical motivations to study Dirac neutrinos include the conservation of global lepton number, a common mass generation mechanism for all Fermion fields, and a clearer distinction between matter and antimatter, which could aid in explaining CP violation in nature [38, 39].

To obtain Dirac neutrinos, three right-handed neutrinos are added to the SM of particles and fields (one for each family), enabling the most general possible Hermitian Dirac mass matrix in the neutral lepton sector in our study. Subsequently, after using a weak basis transformation (WBT) to eliminate nonphysical phases in the Hermitian neutral mass matrix, we aim to fit the mass-squared differences and the mixing angles in the U_{PMNS} matrix, values well measured in neutrino physics thus far, into the parameters.

In our analysis, we assume a diagonal charged lepton mass matrix in the weak basis, which implies that the mixing angles in U_{PMNS} are pure oscillation parameters with no relation with charged lepton mixing. Thus, the unitary matrix that diagonalizes the neutral mass matrix is the same U_{PMNS} , and then, by introducing texture zeros in the neutral sector, we obtain physical predictions that can be tested numerically.

II. ZERO TEXTURES FOR DIRAC NEUTRINOS

For the analysis that follows, we adopt the following three hypotheses: 1) We extend the electroweak sector of the SM with three right-handed neutrino fields, ($\nu_{\alpha R}$; $\alpha = e, \mu, \tau$); 2) The charged lepton mass matrix is diagonal in the weak flavor basis; 3) Majorana masses are forbidden.

A. Neutrino mass matrix

According to the previous hypothesis, for the charged lepton sector in the flavor basis, we have

$$M_l = \begin{pmatrix} m_e & 0 & 0 \\ 0 & m_\mu & 0 \\ 0 & 0 & m_\tau \end{pmatrix}, \quad (2)$$

which implies that the most general 3×3 mass matrix for the neutrinos, which, owing to the decomposition polar theorem of the matrix algebra [36] we assume to be Hermitian without loss of generality, can be expressed as

$$\begin{aligned} M_\nu &= \begin{pmatrix} m_{\nu_e \nu_e} & m_{\nu_e \nu_\mu} & m_{\nu_e \nu_\tau} \\ m_{\nu_\mu \nu_e} & m_{\nu_\mu \nu_\mu} & m_{\nu_\mu \nu_\tau} \\ m_{\nu_\tau \nu_e} & m_{\nu_\tau \nu_\mu} & m_{\nu_\tau \nu_\tau} \end{pmatrix} \\ &= U_{\text{PMNS}} \begin{pmatrix} m_1 & 0 & 0 \\ 0 & m_2 & 0 \\ 0 & 0 & m_3 \end{pmatrix} U_{\text{PMNS}}^\dagger \\ &= \begin{bmatrix} U_{e1} & U_{e2} & U_{e3} \\ U_{\mu1} & U_{\mu2} & U_{\mu3} \\ U_{\tau1} & U_{\tau2} & U_{\tau3} \end{bmatrix} \begin{bmatrix} m_1 & 0 & 0 \\ 0 & m_2 & 0 \\ 0 & 0 & m_3 \end{bmatrix} \begin{bmatrix} U_{e1}^* & U_{\mu1}^* & U_{\tau1}^* \\ U_{e2}^* & U_{\mu2}^* & U_{\tau2}^* \\ U_{e3}^* & U_{\mu3}^* & U_{\tau3}^* \end{bmatrix} \\ &= \begin{bmatrix} U_{e1} & U_{e2} & U_{e3} \\ U_{\mu1} & U_{\mu2} & U_{\mu3} \\ U_{\tau1} & U_{\tau2} & U_{\tau3} \end{bmatrix} \begin{bmatrix} m_1 U_{e1}^* & m_1 U_{\mu1}^* & m_1 U_{\tau1}^* \\ m_2 U_{e2}^* & m_2 U_{\mu2}^* & m_2 U_{\tau2}^* \\ m_3 U_{e3}^* & m_3 U_{\mu3}^* & m_3 U_{\tau3}^* \end{bmatrix}, \end{aligned} \quad (3)$$

where the mixing matrix U_{PMNS} for Dirac neutrinos is parametrized in the usual form as [40]

$$\begin{aligned} U_{\text{PMNS}} &= \begin{bmatrix} 1 & 0 & 0 \\ 0 & c_{23} & s_{23} \\ 0 & -s_{23} & c_{23} \end{bmatrix} \begin{bmatrix} c_{13} & 0 & s_{13} e^{-i\delta_{\text{CP}}} \\ 0 & 1 & 0 \\ -s_{13} e^{i\delta_{\text{CP}}} & 0 & c_{13} \end{bmatrix} \begin{bmatrix} c_{12} & s_{12} & 0 \\ -s_{12} & c_{12} & 0 \\ 0 & 0 & 1 \end{bmatrix} \\ &= \begin{bmatrix} c_{12} c_{13} & s_{12} c_{13} & s_{13} e^{-i\delta_{\text{CP}}} \\ -s_{12} c_{23} - c_{12} s_{23} s_{13} e^{i\delta_{\text{CP}}} & c_{12} c_{23} - s_{12} s_{23} s_{13} e^{i\delta_{\text{CP}}} & s_{23} c_{13} \\ s_{12} s_{23} - c_{12} c_{23} s_{13} e^{i\delta_{\text{CP}}} & -c_{12} s_{23} - s_{12} c_{23} s_{13} e^{i\delta_{\text{CP}}} & c_{23} c_{13} \end{bmatrix}; \end{aligned} \quad (4)$$

where $Dg.(m_1, m_2, m_3)$ represents the neutrino mass eigenvalues, and $c_{ij} = \cos\theta_{ij}$ and $s_{ij} = \sin\theta_{ij}$ are the cosine and sine, respectively, of the mixing angle θ_{ij} , $i < j = 1, 2, 3$.

Now, owing to the Hermiticity constraint, the elements of M_ν satisfy $m_{\nu_e\nu_e} = m_{\nu_e\nu_e}^*$, $m_{\nu_\mu\nu_\mu} = m_{\nu_\mu\nu_\mu}^*$, $m_{\nu_\tau\nu_\tau} = m_{\nu_\tau\nu_\tau}^*$, and $m_{\nu_e\nu_\mu} = m_{\nu_e\nu_\mu}^*$; $m_{\nu_\tau\nu_e} = m_{\nu_e\nu_\tau}^*$ and $m_{\nu_\mu\nu_\tau} = m_{\nu_\tau\nu_\mu}^*$.

For our analysis, it is convenient to use the following numerical values for the entries of U_{PMNS} evaluated at 3σ ranges, presented in Ref. [17]:

$$\begin{pmatrix} 0.7838\dots 0.8442 & 0.5135\dots 0.6004 & 0.1901\dots 0.2183 \\ 0.2508\dots 0.4902 & 0.4665\dots 0.6782 & 0.6499\dots 0.7719 \\ 0.3135\dots 0.5471 & 0.4841\dots 0.6927 & 0.6161\dots 0.7434 \end{pmatrix} \quad (5)$$

which include strong correlations between the allowed ranges owing to unitary constraints.

When the mass matrices for the lepton sector are given by (2) and (3), we observe that the Hermitian mass matrix M_ν has six real parameters and three phases that we can use to explain seven physical parameters: the three mixing angles θ_{12} , θ_{13} , and θ_{23} , one CP violating phase δ , and three neutrino masses m_1 , m_2 , and m_3 . Therefore, in principle, we have a redundant number of parameters (two more phases).

Now, at this point, and contrary to the quark sector [41, 37], we cannot introduce texture zeros via the WBT [42–44] in the mass matrix M_ν because it will change the charged lepton diagonal mass matrix. However, as shown in the appendix, the WBT can be used to eliminate the two redundant phases.

When the redundant phases are removed via the WBT, the Hermitian matrix M'_ν has six real parameters and one phase that can accommodate, in principle, the three mixing angles, three neutrino masses, and CP violation phase. Thus, one texture zero should imply a relationship between the mixing angles and physical masses.

However, we do not have six experimental entries to input in the analysis because the neutrinos masses are not known. Instead, we know the mass square differences $\Delta m_{32}^2 = m_3^2 - m_2^2$; $\Delta_{31}^2 = m_3^2 - m_1^2$, and $\Delta m_{21}^2 = m_2^2 - m_1^2$ in normal hierarchy, with the mathematical constraint $\Delta m_{21}^2 + \Delta m_{32}^2 - \Delta m_{31}^2 = 0$, which leaves us with only five experimental real constraints to be accommodated. Therefore, patterns with one texture zero should, in principle, be compatible with the experimental data at the 3σ level, although the parameter space for each of these zero textures should be strictly constrained (an analysis presented somewhere else). Therefore, real physical predictions should begin only when two texture zeros are considered.

B. Texture zeros

The introduction of texture zeros in a general mass

matrix has been an outstanding hypothesis that provides relationships between the mixing angles and mass values.

As discussed earlier, the six real mathematical parameters of the most general Hermitian mass matrix for Dirac neutrinos provides sufficient room to accommodate the five real experimental values with no prediction. Furthermore, one texture zero should not conduce to any prediction. Therefore, texture zeros become valuable when two of them are introduced, with two texture zeros providing one physical prediction.

In the following, for normal ordering, we study all the possible cases of two texture zeros in the Hermitian mass matrix of Dirac neutrinos and observe the prediction for the lightest Dirac neutrino mass, which consequently has the knowledge of the complete neutrino mass spectrum.

Three different cases must be analyzed: two texture zeros in the diagonal, one texture zero in the diagonal and the other outside the diagonal, and finally two off-diagonal texture zeros.

To set our mathematical notation, we begin studying the implications of one texture zero.

1. Diagonal texture zeros

Let us assume that $m_{\nu_e\nu_e} = 0$ and observe its implications:

From (3), we obtain

$$m_{\nu_e\nu_e} = m_1|U_{e1}|^2 + m_2|U_{e2}|^2 + m_3|U_{e3}|^2 = 0, \quad (6)$$

dividing by m_3 and using the unitary constraint of matrix U , that is $|U_{e1}|^2 + |U_{e2}|^2 + |U_{e3}|^2 = 1$, we can express (6) as

$$\frac{m_1}{m_3}|U_{e1}|^2 + \frac{m_2}{m_3}|U_{e2}|^2 + 1 - |U_{e1}|^2 - |U_{e2}|^2 = 0;$$

which we can rearrange as

$$|U_{e2}|^2 = \frac{m_3}{m_3 - m_2} - \frac{m_3 - m_1}{m_3 - m_2}|U_{e1}|^2. \quad (7)$$

Similarly for $m_{\nu_\mu\nu_\mu} = 0$, we have

$$|U_{\mu 2}|^2 = \frac{m_3}{m_3 - m_2} - \frac{m_3 - m_1}{m_3 - m_2}|U_{\mu 1}|^2, \quad (8)$$

and for $m_{\nu_\tau\nu_\tau} = 0$, we have

$$|U_{\tau 2}|^2 = \frac{m_3}{m_3 - m_2} - \frac{m_3 - m_1}{m_3 - m_2}|U_{\tau 1}|^2. \quad (9)$$

The former three cases can be summarized as

$$|U_{\alpha 2}|^2 = \frac{m_3}{m_3 - m_2} - \frac{m_3 - m_1}{m_3 - m_2}|U_{\alpha 1}|^2, \quad (10)$$

for $\alpha = e$ if $m_{\nu_e \nu_e} = 0$, $\alpha = \mu$ if $m_{\nu_\mu \nu_\mu} = 0$, and $\alpha = \tau$ if $m_{\nu_\tau \nu_\tau} = 0$. This shows the dependence between two of the U_{PMNS} matrix entries and the neutrino mass values.

2. Texture zeros outside the diagonal

Let us now consider a texture zero outside the diagonal. Let us begin with $m_{\nu_e \nu_\mu} = 0$ (notice that $m_{\nu_\mu \nu_e} = m_{\nu_e \nu_\mu}^* = 0$).

For this scenario, (3) implies that

$$m_{\nu_e \nu_\mu} = m_1 U_{e1} U_{\mu 1}^* + m_2 U_{e2} U_{\mu 2}^* + m_3 U_{e3} U_{\mu 3}^* = 0, \quad (11)$$

which, dividing by m_3 and using the orthogonality condition $U_{e1} U_{\mu 1}^* + U_{e2} U_{\mu 2}^* + U_{e3} U_{\mu 3}^* = 0$, can be expressed as

$$\left(\frac{m_1}{m_3} - 1\right) U_{e1} U_{\mu 1}^* + \left(\frac{m_2}{m_3} - 1\right) U_{e2} U_{\mu 2}^* = 0, \quad (12)$$

multiplying by $U_{e2}^* U_{\mu 2}$ and rearranging, we obtain

$$\left(\frac{m_1}{m_3} - 1\right) U_{e1} U_{\mu 1}^* U_{e2}^* U_{\mu 2} + \left(\frac{m_2}{m_3} - 1\right) |U_{e2}|^2 |U_{\mu 2}|^2 = 0, \quad (13)$$

which we can finally expressed as

$$U_{e1} U_{\mu 1}^* U_{e2}^* U_{\mu 2} + \left(\frac{m_3 - m_2}{m_3 - m_1}\right) |U_{e2}|^2 |U_{\mu 2}|^2 = 0, \quad (14)$$

which, together with its complex conjugate, can be separated in two parts: a real part and an imaginary part both equal to zero (note that for a Hermitian matrix, its eigenvalues must be real but not necessarily positive).

As $m_{\nu_\mu \nu_e}$ must also be equal to zero, the two relations must also be equivalent to making the real and imaginary parts in (14) equal to zero. As the second term in (14) is real, making the imaginary part equal to zero produces

$$\text{Im.}(U_{e1} U_{\mu 1}^* U_{e2}^* U_{\mu 2}) = J = 0; \quad (15)$$

which means that this texture zero is associated with a Jarlskog invariant [45] equal to zero, and no CP violation is present for this texture zero.

Similarly for $m_{\nu_e \nu_\tau} = 0$, we have

$$m_{\nu_e \nu_\tau} = m_1 U_{e1} U_{\tau 1}^* + m_2 U_{e2} U_{\tau 2}^* + m_3 U_{e3} U_{\tau 3}^* = 0. \quad (16)$$

Dividing by m_3 and using the orthogonality relationship $U_{e1} U_{\tau 1}^* + U_{e2} U_{\tau 2}^* + U_{e3} U_{\tau 3}^* = 0$, we can express (16) in the form

$$\left(\frac{m_1}{m_3} - 1\right) U_{e1} U_{\tau 1}^* + \left(\frac{m_2}{m_3} - 1\right) U_{e2} U_{\tau 2}^* = 0, \quad (17)$$

multiplying by $U_{e2}^* U_{\tau 2}$ and rearranging, we obtain

$$\left(\frac{m_1}{m_3} - 1\right) U_{e1} U_{\tau 1}^* U_{e2}^* U_{\tau 2} + \left(\frac{m_2}{m_3} - 1\right) |U_{e2}|^2 |U_{\tau 2}|^2 = 0, \quad (18)$$

which implies

$$U_{e1} U_{\tau 1}^* U_{e2}^* U_{\tau 2} + \left(\frac{m_3 - m_2}{m_3 - m_1}\right) |U_{e2}|^2 |U_{\tau 2}|^2 = 0, \quad (19)$$

which again produces

$$\text{Im.}(U_{e1} U_{\tau 1}^* U_{e2}^* U_{\tau 2}) = J = 0. \quad (20)$$

The former means that this texture zero outside the diagonal is also associated with a Jarlskog invariant equal to zero and, again, there is no CP violation for this case.

Similarly, for $m_{\nu_\mu \nu_\tau} = 0$ we obtain

$$m_{\nu_\mu \nu_\tau} = m_1 U_{\mu 1} U_{\tau 1}^* + m_2 U_{\mu 2} U_{\tau 2}^* + m_3 U_{\mu 3} U_{\tau 3}^* = 0, \quad (21)$$

which, divided by m_3 and using the appropriate orthogonality relationship, we obtain

$$\left(\frac{m_1}{m_3} - 1\right) U_{\mu 1} U_{\tau 1}^* + \left(\frac{m_2}{m_3} - 1\right) U_{\mu 2} U_{\tau 2}^* = 0, \quad (22)$$

which, multiplying by $U_{\mu 2}^* U_{\tau 2}$, we obtain

$$U_{\mu 1} U_{\tau 1}^* U_{\mu 2}^* U_{\tau 2} + \left(\frac{m_3 - m_2}{m_3 - m_1}\right) |U_{\mu 2}|^2 |U_{\tau 2}|^2 = 0, \quad (23)$$

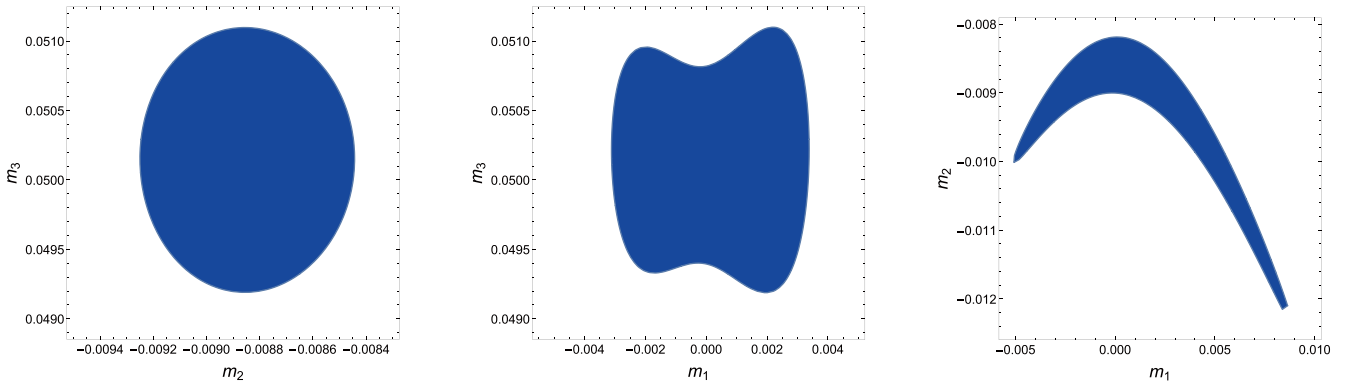
which again yields

$$\text{Im.}(U_{\mu 1} U_{\tau 1}^* U_{\mu 2}^* U_{\tau 2}) = J = 0. \quad (24)$$

Therefore, a texture zero in M_ν outside the main diagonal implies CP conservation, a result also obtained in a different manner in Appendix A.

III. NUMERICAL ANALYSIS

According to (4), the right-hand side of (3) depends only on the neutrino mixing angles, CP-violating phase, and neutrino masses. Therefore, each of the possible six texture zeros in the matrix M_ν in (3) implies an equation relating neutrino masses with the CP-phase and neutrino mixing angles. The equation must be confronted with the measured experimental values. Hence, we must place each equation in terms of physical parameters. Let us observe this:

(a) Plot evaluated at $m_1 = 0.00208$ eV.(b) Plot evaluated at $m_2 = -0.00886$ eV.(c) Plot evaluated at $m_3 = 0.0501$ eV.**Fig. 1.** (color online) Parameter space for the texture zero $M_{\nu_e \nu_e} = 0$ at 95% CL.**A. $m_{\nu_e \nu_e} = 0$**

The texture $m_{\nu_e \nu_e} = 0$ produces the constraint in equation (7), which, when expressed in terms of physical parameters, becomes

$$s_{12}^2 c_{13}^2 = \frac{m_3}{m_3 - m_2} - \frac{(m_3 - m_1)}{(m_3 - m_2)} c_{12}^2 c_{13}^2. \quad (25)$$

This relationship that must be satisfied by experimentally measured values to obtain a realistic texture zero in the neutrino mass matrix.

The relationship (25) can be rearranged slightly by using the definitions $m = m_1 + m_2 + m_3$ and $\Delta m_{32}^2 = m_3^2 - m_2^2$

$$\frac{s_{12}^2 c_{13}^2 \Delta m_{32}^2}{m - m_1} = m_3 - (m_3 - m_1) c_{12}^2 c_{13}^2. \quad (26)$$

The parameter space can be studied through a χ^2 analysis, which is defined as

$$\chi^2(m_1) = \left[\frac{\sin^2 \theta_{12} - \sin^2 \tilde{\theta}_{12}}{\sigma(\sin^2 \theta_{12})} \right]^2, \quad (27)$$

where $\sin^2 \tilde{\theta}_{12}$ is the value for this mixing angle obtained from Eq. (26), whereas $\sin^2 \theta_{12}$ and $\sigma(\sin^2 \theta_{12})$ are the current best fit value and its one sigma deviation, respectively. Experimental data in (1) and (5) are used to perform the analysis.

After defining the parameter space in terms of Δm_{12}^2 , Δm_{13}^2 and the mixing angles θ_{12} , θ_{13} , we perform a minimization process for the χ^2 function. The best fit points obtained around the minimum (about zero) for our analysis are

$$m_1 = 0.00208 \text{ eV}, \quad m_2 = -0.00886 \text{ eV}, \quad m_3 = 0.0501 \text{ eV}.$$

To study the (m_1, m_2, m_3) parameter space, we first fix the m_1 value in its minimum and search for the allowed values of m_2 and m_3 at the 95% confidence level (CL); the results are presented in Fig. 1(a). Next, we fix m_2 in its minimum and search for the allowed values of m_1 and m_3 at the 95% CL, whose results are presented in 1(b). Finally, fixing m_3 , we determine the parameter space allowed for m_1 and m_2 , as presented in Fig. 1(c). The parameter spaces shown in the former three figures satisfy the experimental limits $|m_1| + |m_2| + |m_3| < 0.12$ eV [46], the square mass differences, and the three mixing angles.

Equation (25) shows that the CP violation phase is entirely unconstrained, but the plots in the figure show that the experimentally measured values can be well accommodated in the allowed parameter space, as anticipated above. The mixing angle θ_{23} is easily obtained from the (2,3) or (3,3) mixing matrix numerical entries.

A similar analysis can be performed for the other five one texture zero in the matrix M_ν , that is, for $m_{\nu_\mu \nu_\mu} = 0$, $m_{\nu_\tau \nu_\tau} = 0$, $m_{\nu_e \nu_\mu} = m_{\nu_\mu \nu_e} = 0$, etc. The results for this analysis will be presented elsewhere.

B. Two texture zeros

The next step is to study the different structures with two texture zeros in the neutrino mass matrix (with a diagonal charged lepton sector in the weak basis). We study three different cases: first, the two zeros are in the main diagonal (there are three CP violating patterns); next, one texture zero is in the main diagonal and the other one outside this diagonal (with nine CP conserving different patterns); finally, the two zeros are off the main diagonal (with three CP conserving different patterns).¹⁾

The following section presents, for one particular pat-

1) Other possibilities with two texture zeros in the neutral sector and three texture zeros in the charged sector with at least one of them in the diagonal are analyzed in Refs. [44, 47, 48]

tern, the detailed analytic and numerical analysis for all the different fifteen two texture zeros patterns. Our numerical results are presented in one appendix at the end of the paper.

1. Two zeros, one in the main diagonal

The number of different patterns in this category, all of them related to CP conservation, is nine. They are shown in Appendix B.B.1.

In our analysis, performed in two steps, we reconstruct first the neutrino mass matrix in terms of the three neutrino masses m_1 , m_2 , and m_3 . This is achieved by using the invariant forms: $\text{tr}[M]$, $\text{tr}[M^2]$, and $\text{det}[M]$. Thereafter, we derive the analytic orthogonal matrices that diagonalize the several 3×3 real neutrino mass matrices. The result is the U_{PMNS} in analytic form as a function of the real mass eigenvalues and any other parameter re-

quired, this last one conveniently chosen.

To observe this, let us use as an example here with the texture in A_7 :

$$A_7 = \begin{pmatrix} x_1 & 0 & b \\ 0 & x_2 & c \\ b^* & c^* & 0 \end{pmatrix}. \quad (28)$$

Notice that the three eigenvalues of a general 3×3 Hermitian matrix are real but not necessarily positive. By taking the determinant of A_7 , we obtain $|A_7| = -x_2|b|^2 - x_1|c|^2 = m_1 m_2 m_3$, which by fixing $m_3 > 0$ by a global phase convention, we must have two classes of solutions: $m_1 > 0$, $m_2 < 0$ and $m_1 < 0$, $m_2 > 0$. Let us perform our example for the particular case of $m_1 > 0$ and $m_2 < 0$

After using the invariant forms for this 3×3 mass matrix, and solving the equations, we obtain

$$\begin{pmatrix} x_1 & 0 & \sqrt{\frac{(x_1-m_1)(x_1+m_2)(-x_1+m_3)}{2x_1-m_1+m_2-m_3}} \\ 0 & -x_1+m_1-m_2+m_3 & \sqrt{\frac{(x_1-m_1+m_2)(-x_1+m_1+m_3)(x_1+m_2-m_3)}{2x_1-m_1+m_2-m_3}} \\ \sqrt{\frac{(x_1-m_1)(x_1+m_2)(-x_1+m_3)}{2x_1-m_1+m_2-m_3}} & \sqrt{\frac{(x_1-m_1+m_2)(-x_1+m_1+m_3)(x_1+m_2-m_3)}{2x_1-m_1+m_2-m_3}} & 0 \end{pmatrix}, \quad (29)$$

where m_1, m_2, m_3 , and x_1 are free parameters used to calculate the neutrino masses and mixing angles. After diagonalizing this texture, we obtain the U_{PMNS} in terms of the free parameter.

$$U_{PMNS} = \begin{pmatrix} -\sqrt{\frac{(x_1+m_2)(x_1+m_2-m_3)(m_3-x_1)}{(m_1+m_2)(m_3-m_1)(2x_1-m_1+m_2-m_3)}} & \sqrt{\frac{(x_1-m_1)(x_1-m_1+m_2)(-x_1+m_1+m_3)}{(m_1+m_2)(m_1-m_3)(-2x_1+m_1-m_2+m_3)}} & \sqrt{\frac{(x_1-m_1)(x_1+m_2-m_3)}{(m_1+m_2)(-m_1+m_3)}} \\ -\sqrt{\frac{(m_1-x_1)(m_3-x_1)(-x_1+m_1+m_3)}{(m_1+m_2)(m_2+m_3)(-2x_1+m_1-m_2+m_3)}} & -\sqrt{\frac{(x_1+m_2)(x_1-m_1+m_2)(x_1+m_2-m_3)}{(m_1+m_2)(m_2+m_3)(2x_1-m_1+m_2-m_3)}} & \sqrt{\frac{(x_1+m_2)(-x_1+m_1+m_3)}{(m_1+m_2)(m_2+m_3)}} \\ \sqrt{\frac{(x_1-m_1)(x_1+m_2)(x_1-m_1+m_2)}{(m_1-m_3)(m_2+m_3)(-2x_1+m_1-m_2+m_3)}} & \sqrt{\frac{(x_1-m_3)(x_1-m_1-m_3)(x_1+m_2-m_3)}{(m_1-m_3)(m_2+m_3)(-2x_1+m_1-m_2+m_3)}} & \sqrt{\frac{(x_1-m_1+m_2)(x_1-m_3)}{(m_1-m_3)(m_2+m_3)}} \end{pmatrix}.$$

After obtaining this expression, we conduct a χ^2 minimization procedure:

$$\chi^2(m_1, x_1) = \sum_{i < j} \left[\frac{\sin^2 \theta_{ij} - \sin^2 \tilde{\theta}_{ij}}{\sigma(\sin^2 \theta_{ij})} \right]^2, \quad \text{with } i, j = 1, 2, 3. \quad (30)$$

where $\sin^2 \tilde{\theta}_{ij}$ represents the angles mixing predicted by our forms, whereas $\sin^2 \theta_{ij}$ and $\sigma(\sin^2 \theta_{ij})$ are the current best-fit value and its one sigma deviation, respectively. To obtain the best values that fit the experimental data. Note that the analytical results contain some square root terms that imply several limits on the parameters, such that the results are real; that is, we must have

$$m_3 > x_1 > m_1, \quad 2x_1 > m_3, \quad x_1 + m_2 > m_3.$$

The minimization procedure produces the following phenomenological results: The neutrino masses $|m_1| = 0.0333$ eV, $|m_2| = 0.0344$ eV, $|m_3| = 0.0608$ eV, and the mixing angles $\sin^2 \theta_{12} = 0.315$, $\sin^2 \theta_{23} = 0.646$, $\sin^2 \theta_{13} = 0.022$.

The numerical result agrees with the data reported experimentally by the Neutrino Global Fit [17].

The results of the other eight possibilities are shown in Appendix D.

2. Two zeros off the main diagonal

None of the three cases is viable because each one of them is associated with a vanishing oscillation parameter

(for A_{10} , we have $\theta_{13} = 0$, for A_{11} , we have $\theta_{23} = 0$, and for A_{12} , we have $\theta_{12} = 0$). The forms are shown in Appendix B.B.2.

3. Two zeros in the main diagonal

Three different patterns are given by the matrices A_{13} , A_{14} , and A_{15} . Using the invariant forms as before, we obtain complicated analytic expressions for the U_{PMNS} matrix, whose tracking does not reveal much. Therefore, we proceed immediately with the numerical analysis.

Our result shows that none of the three different textures with two zeroes in the main diagonal can reproduce the three measured mixing angles in the U_{PMNS} oscillation matrix.

IV. SUMMARY

In the context of a model with right-handed neutrinos (one for each family) and global lepton number conservation, we perform an analytic and numerical systematic study of the Dirac neutrino Hermitian mass matrix M_ν with two independent texture zeros, under the assumption that the charged lepton sector is diagonal in the weak basis.

Analytic expressions for the entries of M_ν as functions of the three neutrino masses are obtained using the mathematical invariant of a 3×3 matrix. Algebraic expressions are derived to obtain numerical values for the physical parameters via minimization with a χ^2 statistical analysis.

According to our study, the cases compatible with the current experimental data at the 3σ level are A_3 and A_7 (in Appendix B), both of them associated to normal ordering and CP conservation. This is contrary to the results presented in Refs. [49, 50], where the analysis was performed for correlations between two of the three mixing angles. Now, performing our analysis but relaxing the correlation between the angle $\sin\theta_{13}$ with the other two mixing parameters at the 3σ level, the results in Table [3] are obtained, now in agreement with the results reported in the literature [49, 50].

A new feature in our analysis is the iterative use of WBTs [42–44], which provide the following results: first, the elimination of the two redundant phases in the most general Hermitian neutrino mass matrix ending up with only one physical phase connected with possible CP violation in the lepton sector; second, the demonstration the CP conservation in a novel manner in the context of our analysis when a texture zero outside the main diagonal is placed.

Note that in our analysis, based on the assumption of a diagonal charged lepton mass matrix in the weak basis, our U_{PMNS} matrix is a pure oscillation matrix and not a mixing one as it occurs in the quark sector. This is relevant

because neutrino experiments have measured oscillations.

From our study, the mass for one of the three neutrinos can be predicted (we select the lightest one). Using this value, and the experimental mass squared differences, the entire neutrino mass spectrum can be inferred, as presented in the three tables at the end of the paper. Those values are exact predictions in our analysis. For example, for A_3 in Table D1, we obtain $m_1 = 0.021$, $m_2 = 0.087$, and $m_3 = 0.501$, whose values are predicted in eV.

Although we realized that all the six one zero textures are compatible with current neutrino oscillations, we have not obtained in detail the constraints in the parameter space coming from the experimentally measured values (results presented elsewhere).

Finally, whether neutrinos are Dirac or Majorana particles remains an open question.

APPENDIX A

In this appendix, we address two problems: first, we show how to use the weak basis transformation (WBT) to reduce the number of phases from three to one in a general 3×3 Hermitian neutrino mass matrix (for a diagonal mass matrix in the charged lepton sector). Second, we discuss the mathematical reason for CP conservation when an off-diagonal vanishing element exists in the neutrino sector.

In the context of the SM extended with right-handed neutrinos and lepton number conservation, the most general WBT that leaves the two 3×3 lepton mass matrices Hermitian and does not alter the physics implicit in the weak currents (does not alter the physical content in the U_{PMNS} mixing matrix) is an arbitrary unitary transformation U acting simultaneously in the charged lepton and in the neutrino mass matrices [43]. That is

$$\begin{aligned} M_\nu &\longrightarrow M_\nu^R = U M_\nu U^\dagger, \\ M_l &\longrightarrow M_l^R = U M_l U^\dagger. \end{aligned} \quad (\text{A1})$$

Now, when the mass matrices for the charged lepton sector are diagonal, we have that the most general Hermitian mass matrix M_ν for the neutral sector has six real parameters and three phases that we can use to explain seven physical parameters: three neutrino masses m_1, m_2 , and m_3 , the three mixing angles θ_{12}, θ_{13} , and θ_{23} , and one CP violating phase δ in the U_{PMNS} mixing matrix. Therefore, in principle, we obtain a redundant number of parameters (two more phases).

In contrast to the quark sector [41, 37], we cannot introduce texture zeros via WBTs in the mass matrix M_ν because it would change the charged lepton diagonal mass matrix. However, the WBTs can eliminate the re-

dundant phases. Hence, we express the neutrino mass matrix as

$$M_\nu = \begin{pmatrix} |m_{\nu_e\nu_e}| & |m_{\nu_e\nu_\mu}|e^{i\phi_{e\mu}} & |m_{\nu_e\nu_\tau}|e^{i\phi_{e\tau}} \\ |m_{\nu_e\nu_\mu}|e^{-i\phi_{e\mu}} & |m_{\nu_\mu\nu_\mu}| & |m_{\nu_\mu\nu_\tau}|e^{i\phi_{\mu\tau}} \\ |m_{\nu_e\nu_\tau}|e^{-i\phi_{e\tau}} & |m_{\nu_\mu\nu_\tau}|e^{-i\phi_{\mu\tau}} & |m_{\nu_\tau\nu_\tau}| \end{pmatrix}, \quad (\text{A2})$$

and perform a WBT using the following diagonal unitary matrix:

$$M_\phi = \text{Diag}(e^{i\phi_1}, 1, e^{i\phi_2}), \quad M_\phi^\dagger = \text{Diag}(e^{-i\phi_1}, 1, e^{-i\phi_2}) = M_\phi^{-1},$$

which does not change the diagonal charged lepton mass matrix. After this, the matrix (32) has the following form:

$$M'_\nu = \begin{pmatrix} |m_{\nu_e\nu_e}| & |m_{\nu_e\nu_\mu}|e^{i(\phi_{e\mu}-\phi_1)} & |m_{\nu_e\nu_\tau}|e^{i(\phi_{e\tau}+\phi_2-\phi_1)} \\ |m_{\nu_e\nu_\mu}|e^{-i(\phi_{e\mu}-\phi_1)} & |m_{\nu_\mu\nu_\mu}| & |m_{\nu_\mu\nu_\tau}|e^{i(\phi_{\mu\tau}+\phi_2)} \\ |m_{\nu_e\nu_\tau}|e^{-i(\phi_{e\tau}+\phi_2-\phi_1)} & |m_{\nu_\mu\nu_\tau}|e^{-i(\phi_{\mu\tau}+\phi_2)} & |m_{\nu_\tau\nu_\tau}| \end{pmatrix},$$

where $M'_\nu = M_\phi^\dagger M_\nu M_\phi$. Three cases are present in this expression:

Case A: $\phi_1 = \phi_{e\mu}$ and $\phi_2 = \phi_1 - \phi_{e\tau} = \phi_{e\mu} - \phi_{e\tau}$, producing

$$M'_\nu = \begin{pmatrix} |m_{\nu_e\nu_e}| & |m_{\nu_e\nu_\mu}| & |m_{\nu_e\nu_\tau}| \\ |m_{\nu_e\nu_\mu}| & |m_{\nu_\mu\nu_\mu}| & |m_{\nu_\mu\nu_\tau}|e^{i\psi} \\ |m_{\nu_e\nu_\tau}| & |m_{\nu_\mu\nu_\tau}|e^{-i\psi} & |m_{\nu_\tau\nu_\tau}| \end{pmatrix} \quad (\text{A3})$$

with $\psi = \phi_{\mu\tau} + \phi_2 = \phi_{\mu\tau} + \phi_{e\mu} - \phi_{e\tau}$.

Case B: $\phi_1 = \phi_{e\mu}$ and $\phi_2 = -\phi_{\mu\tau}$, producing

$$M'_\nu = \begin{pmatrix} |m_{\nu_e\nu_e}| & |m_{\nu_e\nu_\mu}| & |m_{\nu_e\nu_\tau}|e^{-i\psi} \\ |m_{\nu_e\nu_\mu}| & |m_{\nu_\mu\nu_\mu}| & |m_{\nu_\mu\nu_\tau}| \\ |m_{\nu_e\nu_\tau}|e^{i\psi} & |m_{\nu_\mu\nu_\tau}| & |m_{\nu_\tau\nu_\tau}| \end{pmatrix}. \quad (\text{A4})$$

Case C: $\phi_2 = -\phi_{\mu\tau}$ and $\phi_1 = \phi_2 + \phi_{e\tau} = \phi_{e\tau} - \phi_{\mu\tau}$, producing

$$M'_\nu = \begin{pmatrix} |m_{\nu_e\nu_e}| & |m_{\nu_e\nu_\mu}|e^{i\psi} & |m_{\nu_e\nu_\tau}| \\ |m_{\nu_e\nu_\mu}|e^{-i\psi} & |m_{\nu_\mu\nu_\mu}| & |m_{\nu_\mu\nu_\tau}| \\ |m_{\nu_e\nu_\tau}| & |m_{\nu_\mu\nu_\tau}| & |m_{\nu_\tau\nu_\tau}| \end{pmatrix}. \quad (\text{A5})$$

From the former, we can conclude that using a WBT, we can eliminate two unwanted phases, obtaining a single phase responsible for the possible CP violation phenomena present in the U_{PMNS} mixing matrix.

Counting parameters once more, we find that in matrix (33) (or equivalently in (34) or (35)), the final number of parameters is six real numbers and one phase (ψ), just sufficient to accommodate the three mixing angles θ_{12}, θ_{13} , and θ_{23} and the three neutrino masses m_1, m_2 , and

m_3 , together with just one CP violating phase to consider the CP violation in the U_{PMNS} matrix via the parameter (δ_{CP}) for Dirac neutrinos. Further texture zeros will reveal relationships between neutrino masses and mixing parameters.

Thus, one texture zero would enable us to express one of the mixing angles θ_{ij} as a function of the neutrino masses; meanwhile, two texture zeros enable us to express two mixing angles as a function of the three neutrino masses. Three or more texture zeros are meaningless.

The most important consequence of the former analysis is that, because the phases ϕ_1 and ϕ_2 are arbitrary and they can take any value, the final phase ψ can be placed in any entry of the neutrino mass matrix, according to (33)–(35). In particular, if we impose an off-diagonal vanishing element, we can place the phase ψ in that entry, meaning that a phase will not be present in the mass matrix. That implies CP conservation for that case. This is a result obtained from the Jarlskog invariant analysis as shown in the main text.

APPENDIX B

As mentioned in the main text, the mass matrix M_ν for Dirac neutrinos, in the context of the SM enlarged with the right-handed neutrinos, can be transformed to be Hermitian without loss of generality, which means that three independent off-diagonal matrix elements are generally complex, whereas the three independent diagonal ones are real. If n of them are taken to vanish (n independent texture zeros), then a combinatorial analysis enables us to express the number of independent matrices as [50]

$$C_n = \frac{6!}{n!(6-n)!}, \quad (\text{B1})$$

which means $C_1 = 6$, $C_2 = 15$, and $C_3 = 20$ (Textures with

$n \geq 3$ are not realistic).

A. One texture zero

Two different scenarios occur: texture zero in the main diagonal and texture zero off the main diagonal, with three different cases for each scenario:

1. Diagonal texture zero

Three different cases are given by the three matrices

$$\begin{aligned} O_1 &= \begin{pmatrix} 0 & a & b \\ a^* & x_2 & c \\ b^* & c^* & x_3 \end{pmatrix}, \\ O_2 &= \begin{pmatrix} x_1 & a & b \\ a^* & 0 & c \\ b^* & c^* & x_3 \end{pmatrix}, \\ O_3 &= \begin{pmatrix} x_1 & a & b \\ a^* & x_2 & c \\ b^* & c^* & 0 \end{pmatrix}, \end{aligned} \quad (\text{B2})$$

with all three cases related to CP violation.

2. Off diagonal texture zero

Again, three different cases are given by the matrices

$$\begin{aligned} O_4 &= \begin{pmatrix} x_1 & 0 & b \\ 0 & x_2 & c \\ b^* & c^* & x_3 \end{pmatrix}, \\ O_5 &= \begin{pmatrix} x_1 & a & 0 \\ a^* & x_2 & c \\ 0 & c^* & x_3 \end{pmatrix}, \\ O_6 &= \begin{pmatrix} x_1 & a & b \\ a^* & x_2 & 0 \\ b^* & 0 & x_3 \end{pmatrix}, \end{aligned} \quad (\text{B3})$$

with all of them related to CP conservation.

B. Two texture zeros

Fifteen different cases are grouped in three different categories:

1. One diagonal and other off-diagonal texture zeros

Nine different cases occur:

$$A_1 = \begin{pmatrix} 0 & 0 & b \\ 0 & x_2 & c \\ b^* & c^* & x_3 \end{pmatrix},$$

$$A_2 = \begin{pmatrix} 0 & a & 0 \\ a^* & x_2 & c \\ 0 & c^* & x_3 \end{pmatrix},$$

$$A_3 = \begin{pmatrix} 0 & a & b \\ a^* & x_2 & 0 \\ b^* & 0 & x_3 \end{pmatrix}, \quad (\text{B4})$$

$$A_4 = \begin{pmatrix} x_1 & 0 & b \\ 0 & 0 & c \\ b^* & c^* & x_3 \end{pmatrix},$$

$$A_5 = \begin{pmatrix} x_1 & a & 0 \\ a^* & 0 & c \\ 0 & c^* & x_3 \end{pmatrix},$$

$$A_6 = \begin{pmatrix} x_1 & a & b \\ a^* & 0 & 0 \\ b^* & 0 & x_3 \end{pmatrix}, \quad (\text{B5})$$

$$A_7 = \begin{pmatrix} x_1 & 0 & b \\ 0 & x_2 & c \\ b^* & c^* & 0 \end{pmatrix},$$

$$A_8 = \begin{pmatrix} x_1 & a & 0 \\ a^* & x_2 & c \\ 0 & c^* & 0 \end{pmatrix},$$

$$A_9 = \begin{pmatrix} x_1 & a & b \\ a^* & x_2 & 0 \\ b^* & 0 & 0 \end{pmatrix}, \quad (\text{B6})$$

with all of them CP conserving.

2. Two texture zeros off the main diagonal

Three different cases occur:

$$A_{10} = \begin{pmatrix} x_1 & a & 0 \\ a^* & x_2 & 0 \\ 0 & 0 & x_3 \end{pmatrix},$$

$$A_{11} = \begin{pmatrix} x_1 & 0 & b \\ 0 & x_2 & 0 \\ b^* & 0 & x_3 \end{pmatrix},$$

$$A_{12} = \begin{pmatrix} x_1 & 0 & 0 \\ 0 & x_2 & c \\ 0 & c^* & x_3 \end{pmatrix}.$$

All of them are related to CP conservation.

3. Two texture zeros in the main diagonal

Three different cases occur:

$$A_{13} = \begin{pmatrix} 0 & a & b \\ a^* & 0 & c \\ b^* & c^* & x_3 \end{pmatrix},$$

$$A_{14} = \begin{pmatrix} 0 & a & b \\ a^* & x_2 & c \\ b^* & c^* & 0 \end{pmatrix},$$

$$A_{15} = \begin{pmatrix} x_1 & a & b \\ a^* & 0 & c \\ b^* & c^* & 0 \end{pmatrix}.$$

All of them related to CP violation.

APPENDIX C

In this appendix, we review the definition of the Jarlskog invariant.

The Swedish physicist Cecilia Jarlskog observed that the area of each of the six unitary triangles in a unitary matrix 3×3 (which is the same for all of them) is given by the relation:

$$-Ar = J/2,$$

where $-J$ is known as the Jarlskog invariant [45], which, in the parametrization that makes use of the Euler angles takes the form

$$-J = c_{12}c_{23}c_{13}^2 s_{12}s_{23}s_{13} \sin \delta_{13}, \quad (C1)$$

which can also be expressed as

$$-|J| = \text{Im}(U_{ij}U_{kl}U_{kj}U_{il}), \quad (C2)$$

for any combination of i, j, k, l , where $i \neq k$ and $j \neq l$.

Thus, the Jarlskog invariant is an important information carrier for CP-violation [51].

APPENDIX D

In this appendix, we present the summary of the numerical results obtained from our analysis for the nine cases of two texture zeroes, one in the main diagonal and the other one outside of it. For the analysis, we use $\delta_{\text{CP}} = 0$. From the results, normal ordering is suggested. Three tables are presented:

The first one corresponds to the analysis for $m_1 > 0$ and $m_2 < 0$. The second is for $m_1 < 0$ and $m_2 > 0$. The third table presents the results obtained when we relax the constraints imposed by the value θ_{13} ; that is, without having a correlation on the $\sin \theta_{13}$ mixing angle with the other parameters.

Table D1 shows that only the texture A_7 can accommodate the measured mixing angles, with the corresponding predictions for the neutrinos mass values.

Table D1. Results of the mixing angles and neutrino masses for the nine different textures obtained according to our analysis for $m_1 > 0$ and $m_2 < 0$.

Texture	$\sin^2 \theta_{12}$	$\sin^2 \theta_{23}$	$\sin^2 \theta_{13}$	$ m_1 /\text{eV}$	$ m_2 /\text{eV}$	$ m_3 /\text{eV}$
1: A_1	0.298	0.250	0.022	0.0018	0.0091	0.0512
2: A_2	0.305	0.018	0.014	0.0044	0.0096	0.0503
3: A_3	0.334	0.007	0.022	0.0021	0.0087	0.0501
4: A_4	0.318	0.200	0.022	0.0046	0.0097	0.0512
5: A_5	0.465	0.010	0.032	0.0153	0.0175	0.0534
6: A_6	0.524	0.003	0.014	0.0209	0.0227	0.0546
7: A_7	0.315	0.646	0.022	0.0333	0.0344	0.0608
8: A_8	0.022	0.515	0.023	0.2685	0.2686	0.2731
9: A_9	0.023	0.516	0.023	0.2765	0.2767	0.2810

Table D2. Results of the mixing angles and the neutrino masses for the nine different textures obtained according to our analysis for $m_1 < 0$ and $m_2 > 0$.

Texture	$\sin^2 \theta_{12}$	$\sin^2 \theta_{23}$	$\sin^2 \theta_{13}$	$ m_1 /\text{eV}$	$ m_2 /\text{eV}$	$ m_3 /\text{eV}$
1: A_1	0.255	0.104	0.022	0.0026	0.0093	0.0599
2: A_2	0.274	0.102	0.023	0.0040	0.0096	0.0513
3: A_3	0.379	0.548	0.022	0.0411	0.0420	0.0649
4: A_4	0.320	0.190	0.022	0.0041	0.0099	0.0508
5: A_5	0.296	0.325	0.020	0.0442	0.0450	0.0665
6: A_6	0.572	0.426	0.021	0.0315	0.0328	0.0600
7: A_7	0.002	0.542	0.021	0.0769	0.0774	0.0920
8: A_8	0.999	0.998	0.517	0.0237	0.0253	0.0557
9: A_9	0.010	0.986	0.511	0.0241	0.0256	0.0553

Table D3. Values of the parameters obtained for the nine different two zero textures for the alternative analysis.

Texture	$\sin^2 \theta_{12}$	$\sin^2 \theta_{23}$	$ m_1 /\text{eV}$	$ m_2 /\text{eV}$	$ m_3 /\text{eV}$
1: A_1	0.320	0.522	0.0077	0.0114	0.0514
2: A_2	0.215	0.318	0.0089	0.0126	0.0508
3: A_3	0.334	0.0146	0	0.0089	0.0497
4: A_4	0.320	0.522	0.0355	0.0365	0.0611
5: A_5	0.230	0.430	0	0.0084	0.0512
6: A_6	0.540	0.020	0.0230	0.0245	0.0551
7: A_7	0.325	0.657	0.0283	0.0297	0.0569
8: A_8	0.318	0.512	0	0.0087	0.0511
9: A_9	0.364	0.909	0.0303	0.0585	0.0585

Table D2 shows that only the texture A_3 can accommodate the measured mixing angles, with the corresponding predictions for the neutrinos mass values.

To compare our results with previous published studies, we conducted an alternative analysis consisting in relaxing the constraint imposed by the value θ_{13} , that is, without having a correlation of the $\sin \theta_{13}$ mixing angle with the other parameters. The results obtained are

presented in Table D3. These values show that textures A_1 , A_4 , A_7 , and A_8 are in fairly good agreement with the experimentally measured numbers at 3σ , resulting in agreement with the analysis already presented in Refs. [49, 50]. Note that when the parameter $\sin \theta_{13}$ is smoothed, we cannot make predictions about all the entries in the U_{PMNS} mixing matrix.

References

- [1] J. F. Donoghue, E. Golowich, and B. R. Holstein *Dynamics of the Standard Model*, Cambridge Monographs on Particle Physics, Nuclear Physics and Cosmology, 2 edition, (Cambridge University Press, 2014)
- [2] P. W. Higgs, *Phys. Rev. Lett.* **13**, 508 (1964)
- [3] S. L. Glashow, *Nucl. Phys.* **22(4)**, 579 (1961)
- [4] S. Weinberg, *Phys. Rev. Lett.* **19**, 1264 (1967)
- [5] C. Giunti and W. K. Chung *Fundamentals of Neutrino Physics and Astrophysics*, 2007
- [6] S. J. Huber and Q. Shafi, *Phys. Lett. B* **498**, 256 (2001)
- [7] R. D. Peccei and H. R. Quinn, *Phys. Rev. Lett.* **38**, 1440 (1977)
- [8] R. N. Mohapatra and G. Senjanović, *Phys. Rev. Lett.* **44**, 912 (1980)
- [9] S. M. Bilenky, J. Hošek, and S. T. Petcov, *Physics Letters B* **94(4)**, 495 (1980)
- [10] T. Mannel, *Nucl. Phys. B Proceedings Supplements* **167**, 170 (2007)
- [11] Y. Fukuda, T. Hayakawa, and *et al.*, *Phys. Rev. Lett.* **81**, 1562 (1998)
- [12] Q. R. Ahmad, R. C. Allen, and *et al.*, *Phys. Rev. Lett.* **89**, 011301 (2002)
- [13] T. Kajita, *Rep. Prog. Phys.* **69(6)**, 1607 (2006)
- [14] B. Abi *et al.* *Deep Underground Neutrino Experiment (DUNE)*, Far Detector Technical Design Report, Volume II : DUNE Physics, 2, 2020
- [15] K. Abe *et al.* *Hyper-Kamiokande Design Report*, 5, 2018
- [16] F. An *et al.* (JUNO Collaboration), *J. Phys. G Nucl. Partic.*

- Phys.* **43**(3), 030401 (2016)
- [17] P. F. De Salas, D. V. Forero, S. Gariazzo *et al.*, *Chi2 profiles from Valencia neutrino global fit*, (2021), <http://globalfit.astroparticles.es/>
- [18] P. F. de Salas, D. V. Forero, S. Gariazzo *et al.*, *JHEP* **02**, 071 (2021)
- [19] P. F. De Salas, S. Gariazzo, O. Mena *et al.*, *Front. Astron. Space Sci.* **5**, 36 (2018)
- [20] S. M. Barr, *Phys. Rev. D* **44**, 3062 (1991)
- [21] M. Gell-Mann, P. Ramond, and R. Slansky, *Conf. Proc. C* **790927**, 315 (1979)
- [22] J. Schechter and J. W. F. Valle, *Phys. Rev. D* **22**, 2227 (1980)
- [23] R. N. Mohapatra and G. Senjanović, *Phys. Rev. D* **23**, 165 (1981)
- [24] P. S. Bhupal Dev and A. Pilaftsis, *Phys. Rev. D* **86**, 113001 (2012)
- [25] Y. Cai, J. Herrero-García, M. A. Schmidt *et al.*, *Front. in Phys.* **5**, 63 (2017)
- [26] M. Agostini *et al.* (GERDA Collaboration), *Phys. Rev. Lett.* **111**(12), 122503 (2013)
- [27] D. Q. Adams *et al.* (CUORE Collaboration), *Phys. Rev. Lett.* **124**(12), 122501 (2020)
- [28] J. B. Albert *et al.* (EXO-200 Collaboration), *Nature* **510**, 229 (2014)
- [29] M. Ratz, M. Lindner and D. Wright, *Phys. Rev Lett.* **84**, 4039 (2000)
- [30] W. Wang, F. wang and J. M. Yamg, *Europhys. Lett.* **76**, 388 (2006)
- [31] E. Ma and R. Srivastava, *Phys. Lett. B* **741**, 217 (2015)
- [32] C. Bonilla, E. Ma, E. Peinado *et al.*, *Phys. Lett., B* **762**, 214 (2016)
- [33] E. Ma and O. Popov, *Phys. Lett. B* **764**, 142 (2017)
- [34] M. Reig, D. Restrepo, J. W. F. Valle *et al.*, *Phys. Rev. D* **97**, 115032 (2018)
- [35] P. Langacker, *Annu. Rev. Nucl. Part. Sci.* **62**, 215 (2012)
- [36] V. Prasolov. *Problems and theorems in linear algebra*. American Mathematical Society. 1 edition, 1994
- [37] A. William, *Eur. Phys. J. C* **71**, 1641 (2011)
- [38] M. C. Gonzalez-Garcia and M. Maltoni, *Phys. Rep.* **460**(1-3), 1 (2008)
- [39] R. N. Mohapatra and A. Y. Smirnov, *Annu. Rev. Nucl. Part. Sci.* **56**, 569 (2006)
- [40] P. A. Zyla *et al.*, *PTEP* **2020**(8), 083C01 (2020)
- [41] W. A. Ponce, J. D. Gómez, and R. H. Benavides, *Phys. Rev. D* **87**(5), 053016 (2013)
- [42] H. Fritzsch and Z.-Z Xing, *Prog. Part. Nucl. Phys.* **45**(1), 1 (2000)
- [43] G. Branco, D. Emmanuel-Costa, R. González Felipe *et al.*, *Phys. Lett. B* **670**(4-5), 340 (2009)
- [44] R. H. Benavides, D. V. Forero, L. Muñoz *et al.*, *Phys. Rev. D* **107**(3), 036008 (2023)
- [45] C. Jarlskog, *Phys. Rev. Lett.* **55**, 1039 (1985)
- [46] N. Aghanim *et al.*, *A&A* **652**, C4 (2021)
- [47] A. Rico, R. H. Benavides, D. V. Forero *et al.*, *PoS ICRC2023*, 1047 (2023)
- [48] R. H. Benavides, Y. Giraldo, L. Muñoz *et al.*, *J. Phys. G* **47**(11), 115002 (2020)
- [49] Y. Lenis, R. Martinez-Ramirez, E. Peinado *et al.*, *Two-zero textures for dirac neutrinos*, 2023
- [50] X. W. Liu and S. Zhou, *J. Mod. Phys. A* **28**, 1350040 (2013)
- [51] I. Esteban, M. C. Gonzalez-Garcia, M. Maltoni *et al.*, *JHEP* **09**, 178 (2020)